SPECTRAL RELAXATION METHOD FOR SOLVING BOUNDARY LAYER EQUATIONS

Thesis Submitted In Partial Fulfillment of The Requirements for
The Award of Degree of
Masters of Science
in
Mathematics & Computing

Submitted by

Parneet Kaur

Roll No.: 301403009

Under the Guidance of
Dr. Raj Nandkeolyar
Assistant Professor

School of Mathematics

THAPAR UNIVERSITY
PATIALA - 147004, INDIA

July, 2016

Certificate

I hereby certify that the work which is being presented in the thesis entitled "**SPECTRAL RELAXATION METHOD FOR SOLVING BOUNDARY LAYER EQUATIONS**" in partial fulfillment of the requirements for the award of degree of Master of Science in "Mathematics and Computing" to the School of Mathematics, Thapar University, Patiala is an authentic record of my own work studied under the supervision of Dr. Raj Nandkeolyar.

The matter embodied in this thesis has not been submitted by me for the award of any other degree of this or any other University/Institute.

Parneet Kaur
(Roll No. 301403009)

This is to certify that the above statement made by the candidate is correct and true to the best of my knowledge.

Dr. Raj Nandkeolyar
Assistant Professor,
Thapar University, Patiala

Countersigned by

Dr. A. K. Lal
Associate Professor & Head,
School of Mathematics,
Thapar University,
Patiala-147004

Dr. S. S. Bhatia
Dean of Academic Affairs,
Thapar University,
Patiala-147004

Acknowledgements

I find no words to express my indebtedness to my thesis supervisor, Dr. Raj Nandkeolyar, Assistant Professor, Thapar University, Patiala, for his valuable guidance and support throughout my work. I thank him for his constant encouragement and advice he has provided throughout my time as his student.

I would like to express my deep sense of gratitude to Dr. A.K. Lal, Head School of Mathematics, Thapar University, Patiala, for providing the necessary facilities needed for this work and directly or indirectly encouraging me to do work. I am highly grateful to Dr. S. S. Bhatia, Dean of Academics Affairs, for his guidance during by dessertation work. I would also like to thank all the faculty members and administrative staff of School of Mathematics, Thapar University, Patiala who have contributed directly or indirectly to this work.

Life at Thapar University, Patiala has been enjoyable with friends who have been always there for me, listening to me, rejoicing me, complaining and pondering my way throughout my study. I would thank them for their great company.

Last but not the least, I would like to thank my parents and my husband, Ravinder, for their continuous support which inspired me and encouraged me, without them I would not be able to complete my work.

Abstract

The heat transfer characteristics of the working fluid in several devices play important role in the overall efficiency of the system. Some fluids with poor heat transfer characteristics affects the performance of these devices. The performance of these devices may be drastically improved by using nanofluid in place of the traditional working fluids. Due to this reason, now a days, the nanofluids are being used in several industrial and domestic appliances such as chillers and refrigerator, cooling electronics devices etc. The aim of the present thesis is to investigate the flow of a nanofluid over a stretching sheet under the influence of a transverse magnetic field using spectral relaxation method. The governing equations modelling such flows are highly non-linear partial differential equations which were reduced to non-linear ordinary differential equations using suitable transformations and then the approximate solution was obtained by spectral relaxation method.

Chapter 1 is introductory. In this chapter a brief account of the nanofluid and its applications, magnetohydrodynamic flows and its applications, heat transfer, boundary layer, governing equations, boundary conditions, the non-dimensional parameters and the spectral relaxation method is presented .

In chapter 2, the fluid flow problem arising during the flow of a viscous incompressible and electrically conducting fluid over a stretching sheet under the influence of an external magnetic field, internal heat generation, and homogeneous-heterogeneous reactions is revisited using the spectral relaxation method. The same problem was earlier solved by using bvp4c routine of MATLAB. The present results were compared with existing results and were found to be an excellent agreement.

Chapter 3 presents a review of the flow of a viscous incompressible and electrically conducting nanofluid over a stretching sheet under the influence of a transverse magnetic field, non linear thermal convection, viscous and Joule heating, and homogeneous-heterogeneous reactions. The problem which was earlier solved by using successive linearisation method, is now dealt with the spectral relaxation method.

Contents

List of Figures

List of Tables

Dedicated to My Parents

Chapter 1

Introduction

1.1 Nanofluids and their Applications

The heat transmission property of several fluids have considerable implications in the performance of many devices such as in air-conditioning devices, electronic devices, chemical devices, power devices etc. The heat transfer properties in many of these applications have been restricted by the use of traditional heat transfer fluids such as water, ethylene glycol, mineral oils etc. These traditional heat transfer fluids have limited heat transfer ability. The use of nanofluids due to the requirement of higher heat transfer capacity in these heat transfer devices. The word nanofluid was termed by Choi.[2] in 1995 which he used for the fluids with suspended nanometer sized ($10^{-9}nm$) particles, called nanoparticles, which where dispersed in some base fluid like water, ethylene glycol etc. The nanoparticles are in general solid nanometer sized particles of metals such as, Al, Cu, Ag, Au, Fe, non-metals such as, Graphite, Carbon nanotubes, oxides such as, $Al_2O_3, Cuo, TiO_2, SiO_2$, Carbides, nitride etc. Later, Choi et al.[3], in their laboratory experiment concluded that the heat transfer characteristics such as thermal conductivity, thermal diffusivity, viscosity and convective heat transfer rates can be altered by nearly dispersing some volume of nanoparticles in to it. This phenomena of heat transfer from nanofluid was also observed by several other researchers [4–9].

There are basically two methods for synthesizing nanofluids for industrial uses. These methods are commonly knows as the single-step method, in which the nanoparticles are directly vaporized in to the base fluid, and the two-step method, in which either the inert gas-condensation or chemical vapor deposition method is used to prepare the nanoparticles which are then dispersed in to the base fluid. The later method is more commonly used for preparing nanofluids and the process of making nanoparticles is more often or not based on the inert gas-condensation [10].

TABLE 1.1: Thermo-physical properties of some traditional fluids and nanoparticles

Material	$\rho(kg/m^3)$	$C_p(J/kgK)$	$k(W/mK)$	$\beta \times 10^{-5}(K^{-1})$	$\sigma(s/m)$
Pure Water	997.1	4179	0.613	21	5.5×10^{-6}
Ethylene glycol	1114	2415	0.252	57	1.07×10^{-6}
Engine oil (EO)	884	1909	0.145	70	1.00×10^{-7}
Mineral Oil	920	1670	0.138	64	1.00×10^{-7}
Blood	1063	3594	0.492	0.18	6.67×10^{-1}
Silver (Ag)	10500	235	429	1.89	6.3×10^{7}
Copper (Cu)	8933	385	401	1.67	5.96×10^{7}
Iron	7870	460	80	58	1.00×10^{7}
Aluminium	2701	902	237	2.31	3.5×10^{7}
Copper Oxide (CuO)	6510	540	18	0.85	5.96×10^{7}
Alumina ($Al2O3$)	3970	765	40	0.85	3.5×10^{7}
Titanium Oxide($TiO2$)	4250	686.2	8.9538	0.9	2.38×10^{6}
Iron Oxide ($Fe3O4$)	5180	670	80.4	20.6	1.12×10^{5}

Nanofluids have some exceptional distinctive features which make them useful in many fluid engineering devices. These feature include their higher thermal conductivity at low nanoparticle aggregation, strong temperature dependent thermal conductivity, non-linear increase in thermal conductivities, nanoparticle concentration and increase in boiling critical heat flux. These distinctive features make nanofluid more useful in industrial and engineering applications including nuclear reaction cooling, geothermal power extraction, automobile fuels, radiator cooling, cooling of electronic devices, smart fluids and in bio and pharmaceutical industry.

1.2 Magnetohydrodynamic Flows and their Applications

Flow of a viscous fluid under the influence of an external magnetic field falls into the category of magnetohydrodynamic (MHD) flows and the branch of physics/applied mathematics which deals with the theoretical investigation of such fluid flows is known as Magnetohydrodynamics. The word *Magnetohydrodynamics* is a combination of three words, viz. *magneto*-meaning magnetic, *hydro*-meaning water, and *dynamics*-meaning movement. Thus, the subject of Magnetohydrodynamics (MHD) is basically the physical-mathematical framework that concerns with the dynamics of magnetic fields in electrically conducting fluids such as salt-water, liquid metals (such as Mercury, gallium, molten iron) and ionized gases or plasmas (such as solar atmosphere). When the flow of an electrically conducting fluid is subjected to an externally applied or otherwise magnetic field, there appears an electric current and an induced magnetic field. The original magnetic field is affected by the induced magnetic field while the fluid motion gets affected by a force known as *Lorentz force* which appears due to the presence of induced current.

The MHD phenomena described above find applications in several engineering devices outlined below:

1.2.1 MHD Power Generator

In conventional turbogenerators electricity is generated by the motion of the conductor through a magnetic field (Faraday's law). The conductor is moved by a compressible fluid, which expends through a nozzle and transfer its internal energy into the mechanical energy of the conductor which in turn is transformed into electrical energy.

In MHD generators the internal energy of the electrically conducting fluid is converted into electrical energy when its moves through a magnetic field. Unfortunately, extremely high temperatures are required to obtain a practical range of conductivity. This requirement is lowered by adding an easily ionized seed material such as alkali metal or its salt. However, the conductivity of the seeded gas is lost if large temperature drops are permitted to occur through the generator channel. This requires the MHD generator to be a topping unit in a system that uses its exhaust gas to further produce power by more conventional methods.

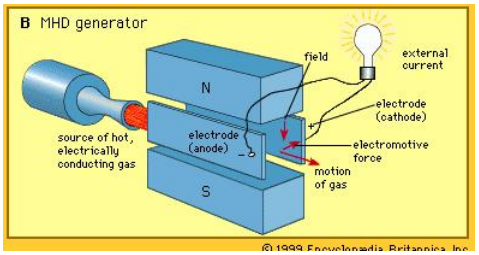

FIGURE 1.1: MHD Generator

1.2.2 MHD Flow Meter

It is an instrument for measurement of ship's speed and is based on the principle that the induced voltage is proportional to the flow rate. This technique is widely used in oceanography.

1.2.3 MHD Submarines

Since at high speeds and deep in the sea the submarines present a lower resistance, they are considered superior to the surface ships. The surface disturbances and formulation of waves are also eliminated in this case, therefore large submarines are considered useful to

transport cargo. MHD submarines obtained their thrust from the Lorentz force produced by transverse electric and magnetic fields, which pump the electrically conducting sea water through or past the submarine [11].

FIGURE 1.2: MHD Propulsion in a Watercraft

1.2.4 Confinement of Plasma in Nuclear Fusion (Pinch Effect)

The confinement of hot plasma is of great importance in nuclear fusion devices where vast amount of energy is released. The magnetohydrodynamics may be used for magnetically pinching the hot plasma. The 'pinch effect,' in its simplest form, is that of a pinching pressure on an infinitely long circular cylinder of plasma exerted by its own circular magnetic field (linear pinch). The plasma carries a current in the longitudinal direction. The current in the plasma produces a circular magnetic field whose center is on the axis of the cylinder and whose plane is at right angle to it. The magnetic field produced by the currents interact with the current to produce a Lorentz force in the radially inward direction, which constricts the plasma particles and keep them away from the vulnerable container walls.

1.2.5 Reentry Problems of Intercontinental Ballistic Missiles ICBM

Plasma sheaths (boundary layer) are formed in front of missiles, in trails of jets from rockets and on surfaces of space vehicles at the time of their reentry the earth atmosphere. The drag of hypersonic vehicles at that time can be increased by the application of MHD drag effects. In MHD boundary layer flow the frictional drag decreases but the magnetic drag increases, resulting in the decrease of heat transfer and increase of the total drag.

1.3 Heat Transfer

The process of exchange of thermal energy between different systems is known as heat transfer. It mainely takes place due to the temperature difference between different systems.

There are three modes of heat transfer between different systems as outlined below :-
(i) Conduction - The process of heat transfer in which the thermal energy is transferred from a hot molecule to its respectively colder neighboring molecule in physical contact is known as conduction.
(ii) Convection - The mode in which heat transfer is caused due to some external forces, for example buoyancy forces, is known as convection.
(iii) Radiation - The mode of heat transfer in which thermal energy between different systems is exchanged using some medium is called Radiation.

The Stefan-Boltzmann law states that, "the emissive power of a black body is directly proportional to fourth power of its absolute temperature". It is represented as:

$$E_b \propto T^4. \tag{1.1}$$

If surface experiences different temperature, then the heat flux is equivalent to the net radiation flow. Using the Rosseland approximation, the radiative heat flux q_r is written as:

$$q_r = -\frac{4\sigma}{3k^*}\frac{\partial T^4}{\partial y}, \tag{1.2}$$

where σ is the Stephan-Boltzmann constant, k^* is the mean absorption coefficient.

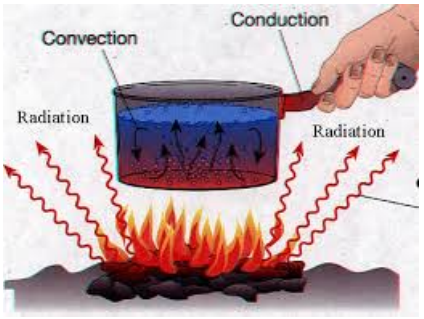

FIGURE 1.3: Modes of Heat Transfer

1.4 Boundary Layers

In a fluid flow problem, the boundary layer is a thin region in the vicinity of the bounding surface where the velocity, temperature and concentration gradients normal to the surface are significant. Beyond this region the variations in the velocity, temperature and concentration are negligible. The thickness of the boundary layer region above the bounding surface is called boundary layer thickness. The boundary layers associated with the velocity, temperature and concentration are commonly known as momentum, thermal and concentration boundary layer, respectively.

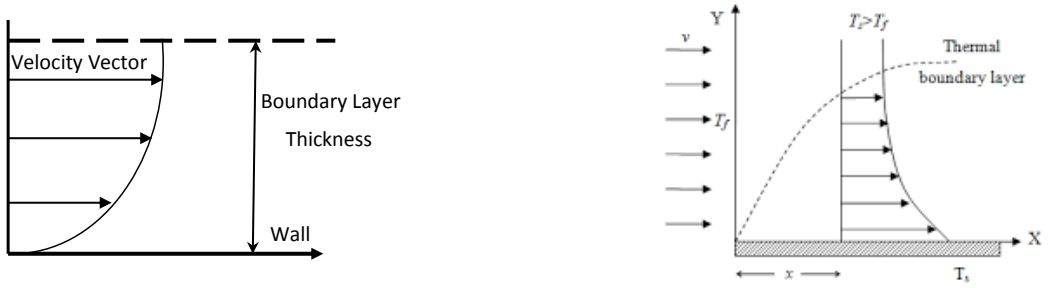

(a) (b)

FIGURE 1.4: Momentum and Thermal Boundary Layers

1.5 Governing Equations

The fluid flow models considerd in the present thesis are governed mainly by two sets of equations, one describing the MHD effects, and the other accounts for the presence of nanofluid.

1.5.1 Basic Equations of Magnetohydrodynamics

The basic equations governing the flow of an electrically conducting fluid under the influence of a magnetic field are the combination of hydrodynamic equations and electrodynamic equations. The properties of electric and magnetic fields are defined by the Maxwell's equations which govern the fundamental laws of electrodynamics. The electrodynamic equations remain as it is but the Ohm's law is modified to include induced current produced by the motion of the fluid. The equation representing the conservation of mass (i.e. the continuity equation) remains as usual but the effects of electric and magnetic fields are to be taken into account to modify the basic laws of fluid-dynamics

comprising conservation of momentum and energy along with the thermal and caloric equations of state. The thermodynamic properties of an electrically conducting fluid remain same as that for non-conducting fluid if we consider fluid as non-magnetic and neglect the phenomena like electrostriction. In Magnetohydrodynamics, when fluid velocity is small compared to the velocity of light, the displacement current is negligible. Also the fluids are almost neutral; the charge density of the fluid and the convection current, being very small compared to the conduction current, can be neglected. Thus the basic equations of Magnetohydrodynamics for the flow of a homogeneous, isotropic, electrically conducting, viscous, incompressible fluid of constant density, constant electrical conductivity and constant kinematic coefficient of viscosity are:

The equation of continuity

$$\nabla.\vec{q} = 0, \tag{1.3}$$

the equation of motion

$$\frac{\partial \vec{q}}{\partial t'} + (\vec{q}\cdot\nabla)\,\vec{q} = -\frac{1}{\rho}\nabla p - \nabla\varphi + \nu\nabla^2\vec{q} + \frac{1}{\rho}\left(\vec{J}\times\vec{B}\right), \tag{1.4}$$

the energy equation

$$\rho c_p\left[\frac{\partial T'}{\partial t'} + (\vec{q}.\nabla)\,T'\right] = k\nabla^2 T' + \psi + \mu\Phi + \frac{J^2}{\sigma}, \tag{1.5}$$

Maxwell's relations

$$\nabla\times\vec{B} = \mu_m\vec{J}, \tag{1.6}$$

$$\nabla\times\vec{E} = -\frac{\partial\vec{B}}{\partial t'}, \tag{1.7}$$

$$\nabla.\vec{B} = 0, \tag{1.8}$$

the constitutive field relation

$$\vec{B} = \mu_m\vec{H}, \tag{1.9}$$

Ohm's law for a moving conductor

$$\vec{J} = \sigma\left[\vec{E} + \left(\vec{q}\times\vec{B}\right)\right], \tag{1.10}$$

where $\vec{q}$ is fluid velocity vector, $\vec{B}$ is magnetic induction vector, $\vec{J}$ is current density vector, $\vec{E}$ is electric field, $\vec{H}$ magnetic field, φ is body force per unit mass including gravitation effects, ψ is thermal radiation or heat generation/absorption term, Φ is viscous dissipation term, T' is fluid temperature, k is thermal conductivity of fluid, μ is kinematic coefficient of viscosity of fluid, c_p is specific heat at constant pressure, μ_m is magnetic permeability of fluid, t' is time, and p is modified pressure including centrifugal

term $-\frac{1}{2}|\Omega\hat{k}\times\vec{r}|^2$, $\vec{r}$ being position vector from the origin to a point at which the Eulerian fluid velocity $\vec{q}$ is measured relative to the rotating frame.
The induction equation for magnetic field is obtained by eliminating $\vec{E}$ and $\vec{J}$ from the equations (1.6), (1.7) and (1.10), and is given by

$$\frac{\partial\vec{B}}{\partial t'} = \nabla\times\left(\vec{q}\times\vec{B}\right) + \upsilon_m\nabla^2\vec{B}. \tag{1.11}$$

where $\upsilon_m = \frac{1}{\sigma\mu_m}$ is the magnetic viscosity or diffusivity.

1.5.2 Basic Equations of Magnetohydrodynamic Nanofluid flow

There are basically two different models to describe the MHD flow of a nanofluid :-

1.5.2.1 The Volume Fraction Model

This model is also known as Maxwell's model and incorporates only the thermophysical properties of the nanoparticles into the system. The governing equations mentioned above essentially remains the same but the thermophysical properties of the base fluid are replaced by the thermophysical properties of nanofluids as mentioned below

The dynamic viscosity of the nanofluid, given by Brinkman [12], is

$$\mu_{nf} = \frac{\mu_f}{(1-\phi)^{2.5}}, \tag{1.12}$$

where ϕ is the solid volume fraction of nanoparticles.

The effective density ρ_{nf} and thermal diffusivity α_{nf} of the nanofluid is defined as [13]

$$\rho_{nf} = (1-\phi)\rho_f + \phi\rho_s. \tag{1.13}$$

$$\alpha_{nf} = \frac{k_{nf}}{(\rho c_p)_{nf}}, \tag{1.14}$$

where k_{nf} is the thermal conductivity of the nanofluid which is given by [14, 15]

$$\frac{k_{nf}}{k_f} = \frac{k_s + 2k_f - 2\phi(k_f - k_s)}{k_s + 2k_f + 2\phi(k_f - k_s)}, \tag{1.15}$$

and the heat capacitance of the nanofluid is given by

$$(\rho c_p)_{nf} = (1-\phi)(\rho c_p)_f + \phi(\rho c_p)_s. \tag{1.16}$$

Here the subscripts nf, f and s refer to the thermophysical properties of the nanofluid, base fluid and nano solid particles, respectively. This model does not include the effects of Brownian diffusion and thermophoretic diffusion which arise due to the presence of nanoparticles.

1.5.2.2 The Brownian motion and thermophoretic diffusion model

This model includes the two effects neglected in the above model. In this model the energy equation is modified as to include these two effects.

The energy equation

$$(\rho c_p)_{nf}\left[\frac{\partial T}{\partial t} + (\vec{q}.\nabla)\,T\right] = k_{nf}\nabla^2 T + \tau\left[D_b \nabla T.\nabla C + \frac{D_T}{T_\infty}\nabla T.\nabla T\right] + \psi + \mu\Phi + \frac{J^2}{\sigma}, \tag{1.17}$$

The nanoparticle mass transfer equation

$$\frac{\partial C}{\partial t} + (q.\nabla)C = D_b\nabla^2 C + \frac{D_T}{T_\infty}\nabla^2 T, \tag{1.18}$$

where D_b is the Brownian diffusion coefficient, D_T is the thermophoretic diffusion coefficient.

1.6 Boundary Conditions

In the present thesis, the governing partial differential equations modeling the flow and heat transfer characteristics of nanofluid has been solved using suitable boundary conditions of Dirichlet, Neumann or mixed type at the surface of the sheet and at the fluid at infinity.

1.6.1 Conditions for Fluid Velocity

If the cohesive forces within the fluid are weaker than the adhesive forces between the fluid and bounding surface then we employ the usual no-slip conditions for the fluid

velocity, i.e, at the bounding surface

$$\vec{q} = \vec{q}_w. \tag{1.19}$$

However, if the cohesive forces are comparatively smaller than the adhesive forces then we use the following partial-slip condition at the bounding surface.

$$\vec{q} = \vec{q}_w + L\left(\frac{\partial \vec{q}}{\partial n}\right), \tag{1.20}$$

where $\vec{q}_w$ is the velocity bounding surface and L is the slip-length.

The fluid velocity far from the boundary surface has the value

$$\vec{q} = \vec{q}_\infty \tag{1.21}$$

where $\vec{q_\infty}$ denote the velocity vector at infinity.

1.6.2 Conditions for Fluid Temperature

If the temperature of the surface is denoted by T_w, the fluid temperature in a layer immediately in contact with the surface will have the same temperature i.e., at the surface

$$T = T_w. \tag{1.22}$$

If the wall is adiabatic then, the boundary condition at the surface becomes

$$\left(\frac{\partial T}{\partial n}\right)_w = 0. \tag{1.23}$$

In case the wall is convectively heated, them using Newton's law of heating or cooling we mention the boundary condition at the surface as

$$-k\left(\frac{\partial T}{\partial n}\right)_w = h(T_f - T), \tag{1.24}$$

where k is the thermal conductivity, h is the heat transfer coefficient, and T_f is the temperature of the fluid. The conditions at free-stream i.e., the conditions out side the boundary layer region are usually taken as

$$T = T_\infty. \tag{1.25}$$

1.7 The Non-dimensional Parameters

During the theoretical investigation of fluid flow problem, one may encounter several non-dimensional parameters. A few of these parameters are outlined below :-

1.7.1 Reynolds Number

The dimensionles quantity Re defined as

$$Re = \frac{UL\rho}{\mu} = \frac{UL}{\nu} \tag{1.26}$$

where U, L, ρ and μ are some characteristic values of the velocity, length, density and viscosity of the fluid respectively, is known as the Reynolds number in honor of the British Scientist Osborne Reynolds, who in 1883 demonstrated the important of Re in the dynamics of viscous fluids. One may note that

$$Re = \frac{UL}{\nu} = \frac{\rho U^2/L}{\mu U/L^2} \approx \frac{\text{Inertial force}}{\text{Viscous force}} \tag{1.27}$$

For this reason Reynolds number is sometime spoken of as the ratio of inertial to viscous forces. It is in fact a parameter for viscosity, for if Re is small the viscous forces will be predominant and the effect of viscosity will be felt in the whole flow field. On the other hand if Re is large the inertial forces will be predominant and in such a case the effect of viscosity can be considered to be confined in a thin layer, known as velocity boundary layer, adjacent to a solid boundary. However, if Re is very large, the flow ceases to be laminar and becomes turbulent.

1.7.2 Prandtl Number

The ratio of the Kinematic viscosity to the thermal diffusivity of the fluid, i.e.,

$$Pr = \frac{\mu c_p}{k} = \frac{\mu/\rho}{k/\rho c_p} = \frac{\nu}{\alpha} = \frac{\text{Kinematic viscosity}}{\text{thermal diffusivity}}, \tag{1.28}$$

is designated as the Prandtl number named after the German scientist Ludwig Prandtl. It is a measure of the relative importance of heat conduction and viscosity of the fluid. The Prandtl number, like the viscosity and thermal conductivity, is a material property and it thus varies from fluid to fluid. For air $Pr = 0.7$ (approx.) and for water at $60°F$, $Pr = 7.0$ (approx.). For liquid metals the prandtl number is very small, e.g., for mercury $Pr = 0.044$, but for highly viscous fluids it may be very large, e.g., for glycerine $Pr = 7250$.

1.7.3 Eckert Number

The dimensionless quantity Ec defined as

$$Ec = \frac{U^2}{c_p T}, \tag{1.29}$$

where U, c_p and T are some reference values of the velocity, specific heat at constant pressure and the temperature, is know as the Eckert number named after the German scientist E.R.G. Eckert.

1.7.4 Grashoff Number

The dimensionless quantity Gr which characterizes the free convection is known as the Grashoff number and is defined as

$$Gr = \frac{gL^3(T_w - T_\infty)}{\nu^2 T_\infty} \tag{1.30}$$

where g is the acceleration due to gravity and T_w and T_∞ are two representative temperatures.

1.7.5 Magnetic Parameter

The 'magnetic parameter' M is defined as

$$M = \mu_e H \sqrt{\frac{\sigma L}{\rho U}} = \sqrt{(Re_H Re_\sigma)} \tag{1.31}$$

It may be easily seen from the equation of motion that magnetic force is of the order of $\sigma\mu_e^2 UH^2$ and the inertial force is of the order of $\rho U^2/L$. Therefore,

$$M^2 = \frac{\sigma\mu_e^2 UH^2}{\rho U^2/L} \approx \frac{\text{magnetic force}}{\text{inertial force}} \tag{1.32}$$

Thus M gives an idea of the importance of magnetic force relative to the inertial force.

1.7.6 Biot Number

Biot number is appears convective heating of the bounding surface. it is defined as:

$$Bi = \frac{h_f L}{k}, \tag{1.33}$$

where, h_f is the heat transfer coefficient, L is the characteristic length, which may be defined as the volume per surface area of the body, k is the thermal conductivity of the body.

1.7.7 Schmidt Number

Schmidt number appears in the system when both momentum and mass diffusion convection simultaneously takes place. This represent the diffusion rate for viscosity with respect to the diffusion rate for mass transfer and defined as :

$$Sc = \frac{\nu}{D_m}, \tag{1.34}$$

where D_m is the mass diffusivity.

1.7.8 Lewis Number

The Lewis number is named after Warren K. Lewis, the first head of the Chemical engineering department at MIT. It is defined at the ratio of thermal diffusion to mass diffusion. i.e.,

$$Le = \frac{\alpha}{D}, \tag{1.35}$$

where D is the mass diffusion. Lewis number is used in the characterization of fluid flow problem where the simultaneous effect of heat and mass transfer take place.

1.8 The Spectral Relaxation Method (SRM)

Consider a system of m non-linear ordinary differential equations in m unknowns functions $z_i(\eta)$ $i = 1, 2, ..., m$ where $\eta \in [a, b]$ is the dependent variable. Define the vector Z_i to be the vector of the derivatives of the variable z_i with respect to η, that is

$$Z_i(\eta) = [z_i^{(0)}, z_i^{(1)}, ..., z_i^{(n_i)}], \tag{1.36}$$

where $z_i^{(0)} = z_i$, $z_i^{(p)}$ is the pth derivative of z_i with respect to η and ni $(i = 1, 2, ...m)$ is the highest derivative order of the variable z_i appearing in the system of equations. The system can be written in terms of Zi as a sum of its linear (Li) and non-linear components (Ni) as

$$L_i[Z_1, Z_2, ..., Z_m] + N_i[Z_1, Z_2, ..., Z_m] = H_i(\eta), i = 1, 2, ..., m, \tag{1.37}$$

where $H(\eta)$ is a known function of η.

For illustrative purposes, we assume that equation (1.37) is to be solved subject to two-point boundary conditions which are expressed as

$$\sum_{j=1}^{m}\sum_{p=0}^{n_j-1}\beta_{\nu,j}^{[p]}z_j^{(p)}(a)=K_{a,\nu}, \qquad \nu=1,2,.....,m_a \tag{1.38}$$

$$\sum_{j=1}^{m}\sum_{p=0}^{n_j-1}\gamma_{\sigma,j}^{[p]}z_j^{(p)}(b)=K_{a,\sigma}, \qquad \sigma=1,2,.....,m_b \tag{1.39}$$

where $\beta_{\nu,j}^{[p]}$, $\gamma_{\sigma,j}^{[p]}$ are the constant coefficients of $z_j^{(p)}$ in the boundary conditions, and m_a, m_b are the total number of prescribed boundary conditions at $\eta = a$ and $\eta = b$ respectively. Starting from an initial approximation $Z_{1,0}, Z_{2,0}, ..., Z_{m,0}$, the iterative technique is obtained as

$$\begin{aligned}
&L_1[Z_{1,r+1}, Z_{2,r}, ..., Z_{m,r}] = H_1 + N_1[Z_{1,r}, Z_{2,r}, ..., Z_{m,r}],\\
&L_2[Z_{1,r+1}, Z_{2,r+1}, Z_{3,r}...., Z_{m,r}] = H_2 + N_2[Z_{1,r+1}, Z_{2,r}, ..., Z_{m,r}],\\
&\qquad\qquad\vdots\\
&L_{m-1}[Z_{1,r+1}, ..., Z_{m-1,r+1}, Z_{m,r}] = H_{m-1} + N_{m-1}[Z_{1,r+1}, ..., Z_{m-2,r+1}, Z_{m-1,r}, Z_{m,r}]\\
&L_m[Z_{1,r+1}, ..., Z_{m-1,r+1}, Z_{m,r+1}] = H_m + N_m[Z_{1,r+1}, ..., Z_{m-1,r+1}, Z_{m,r}],
\end{aligned} \tag{1.40}$$

where $Z_{i,r+1}$ and $Z_{i,r}$ are the approximations of Z_i at the current and the previous iteration, respectively. We note that equation (1.40) forms a system of m linear decoupled equations which can be solved iteratively for $r = 1, 2, ...$, starting from a given initial approximation . The iteration is repeated until convergence is achieved. The desired convergence can be assessed by considering the error due to the decoupling of the governing equations. This decoupling error (Ed) at the $(r+1)th$ iteration is defined using the following formula

$$E_d = Max\left(\|z_{1,r+1} - z_{1,r}\|_\infty, \|z_{2,r+1} - z_{2,r}\|_\infty, ..., \|z_{m,r+1} - z_{m,r}\|_\infty\right) \tag{1.41}$$

The idea used in the development of the iteration scheme (1.40) is imported from the Gauss-Seidel relaxation method for solving large systems of algebraic equations.

Chapter 2

Heat Transfer on Nanofluid Flow with Homogeneous-heterogeneous Reactions and Internal Heat Generation-The SRM Approach

2.1 Introduction

Some heat transfer fluids, such as oil, water, and ethylene glycol mixtures, and poor heat transfer fluids due to their low thermal conductivity. The thermal conductivity of these fluids may be improved by suspending nanosized particle materials in liquid to form a nanofluid. A characteristic feature of the nanofluid is thermal conductivity enhancement [16]. The enhancement in the thermal conductivity of the nanofluid were also confirmed by Xuan and Li [17], Yoo et al.[18], and Hu at al. [19]. As a result, nanofluids are being routinely used in many applications in heat transfer processes, including microelectronics, fuel cells, automobiles, pharmaceutical processes, and hybrid-powered engines, engine cooling/vehicle thermal management, domestic refrigerator, chiller, heat exchanger, nuclear reactor coolant, in grinding, in space technology, defense and ships, and in boiler flue gas temperature reduction [20]. Choi [2] was the first to use the term nano-fluids to refer tot the fluid with suspended nanoparticles. It was observed by Choi et al. [3] that the addition of small amounts(less than 1% by volume) of nanoparticles to conventional heat transfer liquids increases the thermal conductivity of the fluid by approximately two times. Thermophysical properties of nanofluids such as thermal conductivity, diffusivity, and viscosity have been studied by Kang et al.[21], Velagapudi et al. [22], and Rudyak et al. [23]. Makinde and Aziz [24] investigated the boundary layer

flow of a nanofluid past a stretching sheet with a convective boundary condition. They found that with an increase in the Biot number, the concentration layer thickened, but the concentration layer become thinner as the Lewis number increased. Narayana and Sibanda [25] studied the laminar flow of a nanoliquid film over an unsteady stretching sheet.They found that the effectof the nanoparticle volume fraction is to reduce the axial velocity and free stream velocity in the case of a Cu-water nanoliquid, but the opposite was true in the case of Al_2O_3-water nanoliquid. Recently, Kameswaran et al. [26] investigated the hydro-magnetic nanofluid flow due to a stretching or shrinking sheet with viscous dissipation and chemical reaction effects. They found that the velocity profile decreases with an increase in the nanoparticle volume fraction, while the opposite was true in the case of temperature and concentration profiles. They further showed that liquids with nanoparticles suspensions are better suited for the effective cooling of the stretching sheet problem due to their enhanced conductivity and thermal properties. The effects of heat generation/absorption are important in hydro-magnetic fluid flow and heat transfer problems due to their occurrence in many fluid engineering processes. Possible heat generation effects may change the temperature distribution and, therefore, the particle deposition rate. This may occur in such application related to nuclear reactor cores, fire and combustion modeling, electronics chips, and semiconductor wafers. Due to this fact, researchers found the study of heat generation/absorption effects very interesting on the flow of nanofluids past stretching /shrinking sheets. Hamad and Pop [27] investigated the unsteady MHD free convection flow past a vertical permeable flat plate in a rotating frame of reference with constant heat source in a nanofluid. Hamad and Pop [28] applied the scaling transformations to study the boundary layer flow near the stagnation-point on a heated permeable stretching surface in a porous medium saturated with a nanofluid and heat generation/absorption effects. They showed that the addition of nanoparticles to a base fluid changes the flow pattern. Chamkha and Aly [29] studied the heat generation/absorption velocity effect on MHD free convection flow of a nanofluid past a vertical plate. It was shown that an increase in the heat generation causes an increase in the longitudinal velocity and temperature of the nanofluid. Alsaedi et al. [30] studied the effects of heat generation/absorption on stagnation point flow of nanofluid over a surface with convective boundary conditions. Several chemically reacting systems involve both homogeneous and heterogeneous reactions, with examples occurring in combustion, catalysis, and biochemical systems. The interaction between the homogeneous reaction in the bulk of the fluid and heterogeneous reaction occurring on some catalytic surfaces is generally very complex, and is involved in the production and consumption of reactant species at different rates both within the fluid and on the catalytic surfaces. A model for isothermal homogeneous-heterogeneous reactions in boundary layer flow of a viscous fluid past a flat plate was studied by Merkin [31]. He presented the homogeneous reaction by cubic autocatalysis and the heterogeneous reaction by a first order process and

showed that the surface reaction is the dominant mechanism near the leading edge of the plate. Chaudhary and Merkin [32] investigated homogeneous-heterogeneous reactions in boundary layer flow. They obtained the numerical solution near the leading edge of the flat plate. Ziabakhsh et al. [33] studied the problem of flow ad diffusion of chemically reactive species over a nonlinearly stretching sheet immersed in a porous medium. Chambre and Acrivos [34] studied an isothermal chemical reaction on a catalytic reactor in laminar boundary layer flow. They found that the actual surface concentration without introducing unnecessary assumptions related to the reaction mechanics. The effects of flow near the two-dimensional stagnation point flow in an infinite permeable wall with a homogeneous-heterogeneous reaction were studied by Khan and Pop [35]. They solved the governing nonlinear equations using the implicit finite difference method and observed that the mass transfer parameter considerably affects the flow characteristics. Khan and Pop [36] investigated the effects of homogeneous-heterogeneous reactions on a viscoelastic fluid toward a stretching sheet. They observed that the concentration at the surface decreased with an increase in the viscoelastic parameter. Recently, Kameswaran et al. [37] investigated the homogeneous-heterogeneous reactions in a nanofluid flow due to a porous stretching sheet. They showed that the velocity profiles decrease with an increase of nanoparticle volume fraction for both Cu-water and Ag-water nanofluids. The aim of the present review work is to test the efficiency of the spectral relaxation method (SRM) in solving the problem considered by Nandkeolyar et al. [1]. The flow of a viscous incompressible and electrically conducting nanofluid over a stretching sheet is studied considering the effects of an external magnetic field, internal heat generation and homogeneous-heterogeneous reactions. The governing nonlinear partial differential equations are subjected to similarity transformation to obtain a set of nonlinear ordinary differential equations and then the solution of the equation is obtained using SRM method.

2.2 Mathematical Formulation

Consider the steady two dimensional boundary layer flow of a viscous, incompressible, and electrically conducting nanofluid through a stretching sheet in the presence of internal heat generation. A Cartesian coordinate system is used with the x-axis along the sheet and the y-axis normal to the sheet. Two equal but opposite forces are applied along the sheet so that the wall is stretched, melted with a uniform transverse magnetic field B_0. It is assumed that the induced magnetic field produced by the fluid motion is negligible in comparison to the applied one. This assumption is valid for low magnetic Reynolds number fluids [11]. Also, there is no external applied electric field so that the effect of polarization of magnetic field is negligible [38]. The fluid is

a water based nanofluid containing copper(Cu) or gold(Au) nanoparticles. The base fluid and the nanoparticle are in thermal equilibrium and no slip occurs between them. The thermophysical properties of the nanofluid are given. It is assumed that a simple homogeneous-heterogeneous reactions model exists as proposed by Chaudhary and Merkin [32] in the following form:

$$A + 2B \to 3B, \quad rate = k_c ab^2 \tag{2.1}$$

while on the catalyst surface we have the single, isothermal, first order reaction

$$A \to B, \quad rate = k_c a \tag{2.2}$$

where a and b are the concentrations of the chemical species A and B , k_c and k_s are the rate constants. It is assumed that both the reaction processes are isothermal. Under these assumptions, the boundary layer equations describing the nanofluid flow, heat, and mass transfer can be written as

$$\frac{\partial u}{\partial x} + \frac{\partial v}{\partial y} = 0 \tag{2.3}$$

$$u\frac{\partial u}{\partial x} + v\frac{\partial v}{\partial y} = \frac{\mu_{nf}}{\rho_{nf}}\frac{\partial^2 u}{\partial y^2} - \frac{\sigma B_0^2}{\rho_{nf}}u \tag{2.4}$$

$$u\frac{\partial T}{\partial x} + v\frac{\partial T}{\partial y} = \alpha_{nf}\frac{\partial^2 T}{\partial y^2} + \frac{Q_0}{(\rho c_p)_{nf}}(T - T_\infty) \tag{2.5}$$

$$u\frac{\partial a}{\partial x} + v\frac{\partial a}{\partial y} = D_A\frac{\partial^2 a}{\partial y^2} - k_c ab^2 \tag{2.6}$$

$$u\frac{\partial b}{\partial x} + v\frac{\partial b}{\partial y} = D_B\frac{\partial^2 b}{\partial y^2} + k_c ab^2 \tag{2.7}$$

The corresponding boundary conditions are

$$\begin{aligned} &u = u_w = cx, v = 0, T = T_w = T_\infty + C\left(\frac{x}{l}\right)^2, \\ &D_A\frac{\partial a}{\partial y} = k_s a, D_B\frac{\partial b}{\partial y} = -k_s a \quad \text{at} \quad y = 0 \\ &u \to 0, t \to T_\infty, a \to a_0, b \to 0, \quad \text{as} \quad y \to \infty \end{aligned} \tag{2.8}$$

where u and v are the velocity components in the x- and y-directions, respectively, μ_{nf} is the dynamic viscosity of the nanofluid,ρ_{nf} is the density of the nanofluid, σ is the electrical conductivity of the nanofluid, T is the temperature of the nanofluid , Q_0 is the internal heat generation coefficient of the nanofluid, c ist he stretching rate, D_A and D_B are the respective diffusion coefficient of species A and B, a_0 is a positive constant, T_∞ is the temperature of free stream, C is a constant, and l is characteristic length. The

dynamic viscosity of the nanofluid was given by Brinkman [12] as

$$\mu_{nf} = \frac{\mu_f}{(1-\phi)^{2.5}} \tag{2.9}$$

where ϕ is the solid volume fraction of nanoparticles. The effective density of the nanofluid is given as

$$\rho_{nf} = (1-\phi)\rho_f + \phi\rho_s \tag{2.10}$$

The thermal diffusivity of the nanofluid is

$$\alpha_{nf} = \frac{k_{nf}}{(\rho C_p)_{nf}} \tag{2.11}$$

where k_{nf} is the thermal conductivity of the nanofluid, and $(\rho C_p)_{nf}$ is the heat capacitance of the nanofluid, and are defined as

$$\frac{k_{nf}}{k_f} = \frac{k_s + 2k_f - 2\phi(k_f - k_s)}{k_s + 2k_f + 2\phi(k_f - k_s)} \tag{2.12}$$

$$(\rho C_p)_{nf} = (1-\phi)(\rho C_p)_f + \phi(\rho C_p)_s \tag{2.13}$$

Here, the subscripts nf, f and s refer to the thermophysical properties of the nanofluid, base fluid, and nanosolid particles, respectively. The equation of continuity (2.3) is satisfied automatically by introducing a stream function $\varphi(x, y)$ such that

$$u = \frac{\partial \varphi}{\partial y} \text{ and } v = -\frac{\partial \varphi}{\partial x} \tag{2.14}$$

where $\varphi = (c\nu_f)^{1/2} x f(\eta), f(\eta)$ is dimensionless stream function where $\eta = (c/\nu_f)^{1/2} y$. The velocity components are then given by

$$u = cx f^{'}(\eta) \text{ and } v = -(c\nu_f)^{1/2} f(\eta)$$

the temperature of the nanofluid is represented as

$$T = T_\infty + (T_w - T_\infty)\theta(\eta) \tag{2.15}$$

and the concentration of the chemical species A and B are represented as

$$a = a_0 g(\eta) \text{ and } b = a_0 h(\eta) \tag{2.16}$$

where a_0 is a constant, $\theta(\eta)$ is the dimensionless temperature of the nanofluid, and $g(\eta)$ and $h(\eta)$ are dimensionless concentrations. Using Eqs.(2.9)-(2.16), Eqs.(2.4)-(2.8) , in

nondimensionless form, reduce to the following two points boundary value problems

$$f''' + \phi_1 \left(ff'' - \frac{M}{\phi_2} f' - f'^2 \right) = 0 \tag{2.17}$$

$$\theta'' + Pr \frac{k_f}{k_{nf}} \phi_3 \left(f\theta' - 2f'\theta + \frac{\beta}{\phi_3}\theta \right) = 0 \tag{2.18}$$

$$\frac{1}{Sc} g'' + fg' - kgh^2 = 0 \tag{2.19}$$

$$\frac{\delta}{Sc} h'' + fh' + kgh^2 = 0 \tag{2.20}$$

$$f(0) = 0, f'(0) = 1, f'(\eta) \to 0 \ \text{ as } \ \eta \to \infty \tag{2.21}$$

$$\theta(0) = 1, \theta(\eta) \to 0 \ \text{ as } \ \eta \to \infty \tag{2.22}$$

$$g' = K_s g(0), g(\eta) \to 1 \ \text{ as } \ \eta \to \infty \tag{2.23}$$

$$\delta h' = -K_s g(0), h(\eta) \to 0 \ \text{ as } \ \eta \to \infty \tag{2.24}$$

where

$$\phi_1 = (1-\phi)^{2.5} \left[(1-\phi) + \phi \left(\frac{\rho_s}{\rho_f} \right) \right] \tag{2.25}$$

$$\phi_2 = \left[(1-\phi) + \phi \left(\frac{\rho_s}{\rho_f} \right) \right] \tag{2.26}$$

$$\phi_3 = \left[(1-\phi) + \phi \left(\frac{(\rho C_p)_s}{(\rho C_p)_f} \phi \right) \right] \tag{2.27}$$

The nondimensional constants in Eqs (2.17)-(2.24) are the magnetic parameter M, the Prandtl number Pr, the heat generation parameter β, the Schmidt number Sc, the measure of strength of the homogeneous reaction k, the measure of strength of the heterogeneous reaction K_s, and the ratio of diffusion coefficients δ. These are defined as

$$\begin{aligned} &M = \frac{\sigma B_0^2}{\rho_f c}, Pr = \frac{(\rho \mu C_p)_f}{k_f}, \beta = \frac{Q_0}{c(\rho C_p)_f}, \\ &Sc = \frac{\nu_f}{D_A}, k = \frac{k_c a_0^2}{c}, K_s = \frac{k_s}{D_A}\sqrt{\frac{\nu_f}{c}}, \delta = \frac{D_B}{D_A} \end{aligned} \tag{2.28}$$

It is expected that the diffusion coefficient of chemical species A and B are of a comparable size which leads us to make a further assumption that the diffusion coefficient D_A and D_B are equal, i.e., $\delta = 1$ [32]. This assumption leads to the following relation:

$$g(\eta) + h(\eta) = 1 \tag{2.29}$$

Equations (2.19) and (2.20) under this assumption reduce to

$$\frac{1}{Sc} g'' + fg' - kg(1-g)^2 = 0 \tag{2.30}$$

and are subject to the boundary conditions

$$g^{'}(0) = K_s g(0), g(\eta) \to 1 \ \text{ as } \ \eta \to \infty \tag{2.31}$$

2.3 Skin Friction Coefficient

The physical quantity of interest is the skin friction coefficient C_f, which characterizes the surface drag. The shearing stress at the surface of the wall τ_w is given by

$$\tau_w = -\mu_{nf}\left[\frac{\partial u}{\partial y}\right]_{y=0} = -\frac{1}{(1-\phi)^{2.5}}\rho_f\sqrt{\nu_f c^3}xf^{''}(0) \tag{2.32}$$

where μ_{nf} is the coefficient of viscosity. The skin friction coefficient is defined as

$$C_f = \frac{2\tau_w}{\rho_f u_w^2} \tag{2.33}$$

and using Eq.(2.32) in Eq.(2.33) we obtain

$$C_f(1-\phi)^{2.5}\sqrt{Re_x} = -2f^{''}(0) \tag{2.34}$$

where Re_x is the local Reynolds number, which is defined as $Re_x = \frac{xu_w}{\nu_f}$

2.4 Heat Transfer Coefficient

The heat transfer rate at the wall is given by

$$q_w = -k_{nf}\left[\frac{\partial T}{\partial y}\right]_{y=0} = -k_{nf}C\left(\frac{x}{l}\right)^2\sqrt{\frac{c}{\nu_i}}\theta^{'}(0) \tag{2.35}$$

where k_{nf} is the thermal conductivity of the nanofluid. The Nusselt number is defined as

$$Nu_x = \frac{xq_w}{k_f(T_w - T_\infty)} \tag{2.36}$$

Using Eq.(2.35) in Eq.(2.36) the dimensionless wall heat transfer rate is obtained as

$$\frac{Nu_x}{\sqrt{Re_x}}\left(\frac{k_f}{k_{nf}}\right) = \theta^{'}(0) \tag{2.37}$$

2.5 Numerical Technique

The above set of equations (2.17), (2.18) and (2.30) subject to the boundary conditions stated in (2.21), (2.22) and (2.31) were solved using Successive Linearisation Method (SLM) by Nandkeolyar et al.[1] in order to verify the robustness and applicability of Spectral Relaxation Method (SRM) we intend to apply the SRM on the problem studied by Nandkeolyar et al.[1] In view of SRM algorithm the linearised iteration scheme is given by

$$p_{r+1}^{''} + \phi_1 \left(f_{r+1} p_{r+1}^{'} - \frac{M}{\phi_2} p_{r+1} - p_r^2 \right) = 0 \tag{2.38}$$

$$\theta_{r+1}^{''} + \frac{Prk_f}{k_{nf}} \left(f_{r+1} \theta_{r+}^{'} - 2 f_{r+1}^{'} \theta_{r+1} + \frac{\beta}{\phi_3} \theta_{r+1} \right) = 0 \tag{2.39}$$

$$\frac{1}{Sc} g_{r+1}^{''} + f_{r+1} g_{r+1}^{'} - K g_{r+1} = K(g_r^3 - 2g_r^2) \tag{2.40}$$

The boundary conditions for the above iteration scheme are

$$f_{r+1}(0) = 0, f_{r+1}^{'}(0) = 1, f_{r+1}^{'}(\eta) \to 0 \quad \text{as} \quad \eta \to \infty \tag{2.41}$$

$$\theta_{r+1}(0) = 1, \theta_{r+1}(\eta) \to 0 \quad \text{as} \quad \eta \to \infty \tag{2.42}$$

$$g_{r+1}^{'} = K_s g_{r+1}(0), g_{r+1}(\eta) \to 1 \quad \text{as} \quad \eta \to \infty \tag{2.43}$$

In order to solve the decoupled equations (2.38)-(2.40), we use the Chebyshev spectral collocation method. The computational domain $[0, L]$ is transformed to the interval $[-1, 1]$ using $\eta = L(\xi + 1)/2$ on which the spectral method is implemented. Here L is used to invoke the boundary condition at ∞. The basic idea behind the spectral collocation method is the introduction of a differentiation matrix $\mathcal{D}$ which is used to approximate the derivatives of the unknown variable at the collocation points as the matrix vector product of the form

$$\frac{df_{r+1}}{d\xi} = \Sigma_{k=0}^{N} \mathbf{D}_{lk} f_r(\eta_k) = \mathbf{D}\mathbf{f}_r, l = 0, 1, 2, ..., N \tag{2.44}$$

where $N + 1$ is the number of collocation points (grid points), $\mathbf{D} = 2\mathcal{D}/L$, and $f = [f(\eta_0), f(\eta_1, ..., f(\eta_N)]^T$ is the vector function at the collocation points. Higher-order derivatives obtained as poers of D, that is,

$$f_r^{(p)} = \mathbf{D}^p \mathbf{f}_r, \tag{2.45}$$

where p is the order of the derivative. Applying the spectral method to equations (2.38)-(2.40) we obtain

$$A_1 f_{r+1} = B_1 \tag{2.46}$$

$$A_2 p_{r+1} = B_2 \tag{2.47}$$

$$A_3 \theta r + 1 = B_3 \tag{2.48}$$

$$A_4 g_{r+1} = B_4 \tag{2.49}$$

where

$$A_1 = \mathbf{D}$$

$$B_1 = p_r \tag{2.50}$$

$$A_2 = diag\left(\frac{1}{\phi_1}\right)\mathbf{D}^2 + diag(f_{r+1})\mathbf{D} - \frac{M}{\phi_2}I$$

$$B_2 = p_r^2 \tag{2.51}$$

$$A_3 = \mathbf{D}^2 + diag\left(\frac{Prk_f f_{r+1}}{k_{nf}}\right) f_{r+1}\mathbf{D} - diag\left(2f'\frac{Prk_f}{k_{nf}} + \frac{\beta}{\phi_3}\frac{Prk_f}{k_{nf}}\right) I$$

$$B_3 = 0 \tag{2.52}$$

$$A_4 = diag\left(\frac{1}{Sc}\right)\mathbf{D}^2 + diag(f_{r+1})\mathbf{D} - diag(k)I$$

$$B_4 = K(g_r^3 - 2g_r^2) \tag{2.53}$$

In equations(2.63)-(2.66) , I is an identity matrix and diag[ ] is a diagonal matrix, all of size $(N+1)X(N+1)$ where N is the number of grid points,$\mathbf{f}, \mathbf{p}, \theta$ and $\mathbf{g}$ are the values of the functions f, p, θ and g respectively, when evaluated at the grid points and the subscript r denotes the iteration number. The initial guesses to start the SRM scheme for equation (2.50)-(2.53) are chosen as

$$f(\eta) = 1 - e^{-\eta}, \theta = e^{-\eta}, g'(\eta) = \frac{1}{2}K_s e^{-K_s \eta} \tag{2.54}$$

2.6 Numerical Results

In order to study the efficiency of the spectral relaxation method on the present problem, the values of skin friction coefficient $-f''(0)$ and heat transfer coefficient $-\theta'(0)$ were calculated and compared with the old values reported by Nandkeolyar et al. [1]. This comparison is presented in Table 2.1. It is observed that the results obtained using spectral relaxation method are in excellent agreement with the results reported by

TABLE 2.1: Comparison between values of Nandkeolayar et al [1] and present values of skin friction $-f^{''}(0)$ and Nusselt number $-\theta^{'}(0)$ for various values of magnetic parameter M , heat generation parameter β, and solid volume fraction ϕ when $k = K_s = 1$ and $Sc = 5$

			Nandkeolayar et al [1]		Present Values	
M	β	ϕ	$-f^{''}(0)$	$-\theta^{'}(0)$	$-f^{''}(0)$	$-\theta^{'}(0)$
1	0.1	0.1	1.465763	3.104635	1.465763	3.104635
2	0.1	0.1	1.707892	3.033622	1.707892	3.033622
3	0.1	0.1	1.919720	2.969732	1.919720	2.969732
2	0.1	0.1	-	3.033621	-	2.923953
2	0.15	0.1	-	2.983385	-	2.868761
2	0.2	0.1	-	2.931557	-	2.810897
2	0.1	0.0	1.732050	3.608821	1.732050	3.608821
2	0.1	0.1	1.707892	3.033622	1.707892	3.033622
2	0.1	0.2	1.621264	2.581263	1.621264	2.581263

Nandkeolyar et al. [1]. We may further note from Table 2.1 that the skin friction coefficient $-f^{''}(0)$ and rate of heat transfer at the surface $-\theta^{'}(0)$ for different flow parameters we may conclude that an increase in M causes an increase in the skin fraction coefficient while it opposite effect is observed on the rate of heat transfer at the surface for both Cu-water and Au-water nanofluid. An increase in the heat generation parameter β causes a decrease in the rate of heat transfer at the plate. We observed that an increase in the nanoparticle volume fraction causes a decrease in the rate of heat transfer at the plate the nanoparticle volume fraction tends to reduce the skin friction in the case Cu-water nanofluid. The nanoparticle volume fraction has a completely opposite effect on the skin friction in the case of Au-water nanofluid. It may also be noted that the skin friction in the case of Cu-water nanofluid is less then that of the skin friction in the case of Au-water nanofluid whereas the rate of heat transfer is less in the case of Au-water nanofluid as compared to Cu-water nanofluid.

Chapter 3

Viscous and Joule Heating in the Stagnation Point Nanofluid Flow Through a Stretching Sheet-The SRM Approach

3.1 Introduction

In the above studies, the effect of an external applied magnetic field was not considered. However, it is well known that the use of a magnetic field in fluid flow and heat transfer problems provides a stabilization mechanism. Such type of flows is encountered in polymer industry and metallurgy. The metallurgical applications include the cooling of continuous strips or filaments in , for example, the process of drawing, annealing, and thinning of copper wires. However, there are very few studies which considered the effect of an external magnetic field on the stagnation point flow of a nanofluid over a stretching/shrinking sheet. The effect of magnetic field on stagnation point flow and heat transfer due to nanofluid toward a stretching sheet was studied by Ibrahim et al. [39]. The transport equations employed in the analysis included the effect of Brownian motion and thermophoresis. they observed that the presence of transverse magnetic field decreases the velocity field. Chamkha etal. [40] investigated the unsteady, laminar, boundary-layer flow with heat and mass transfer of a nanofluid along a horizontal stretching plate in the presence of a transverse magnetic field, melting, and the heat generation or absorption effects. Beg et al. [41] presented an explicit numerical investigation of unsteady magneto-hydrodynamic (MHD) mixes convective boundary layer flow of a nanofluid over an exponentially stretching sheet in a porous media. They

also observed that the Lorentzian hydro-magnetic tends to retard the flow considerably. Convective heat transfer in flow of nanofluids is important in different engineering devices, where a change in the heat transfer directly causes a change in the flow field. The natural convective boundary layer flow of a nanofluid past a vertical plate was studied by Kuznetsov and Nield [42]. They obtained an analytic solution for the flow and heat transfer problem. Das [43] studied the mixed convection stagnation point flow and heat transfer of a copper-water nanofluid toward a shrinking sheet. Pakravan and Yaghoubi [44] investigated the combined thermophoresis. Brownian motion, and Dufour effects on the natural convection of nanofluids. The double diffusive natural convective boundary-layer flow a nanofluid past a vertical plate is studied by Kuznetsov and Nield [45]. In most of research papers, the effect of buoyancy forces is studied assuming that the temperature and density vary linearly. However, there are several reasons for the density temperature relationship to become nonlinear. Thermal stratification and heat released by viscous dissipation (e.g., wall jets) induce significant changes in density gradient [46]. In such cases, when the temperature difference between the surface of the plate and the ambient fluid becomes significantly large, nonlinear density and temperature variations in the buoyancy force term may exert a strong influence o the flow field. The effect of variable coefficient thermal expansion was investigated by Barrow and Rao [47] and Brown [48]. Partha [46] investigated the natural convection in a non-Darcy porous medium using a temperature-concentration-dependent density relation. He concluded that the effect of a non-linear temperature parameter is much more significant in a Darcy medium as compared with a non-Darcy porous medium. Prasad et al. [49] studied the coupled nonlinearity generated by the density variation with temperature on the non-Darcy porous flow on a vertical flat plate embedded in a fluid saturated porous medium in the presence of the lateral mass flux with prescribed constant surface temperature. In addition to the non-linearity in the density temperature relation, viscous and Joule dissipation effects on such boundary layer flows have a significant impact. The heat transfer characteristics of the flow are directly influenced by these effects which include changes in heat transfer within the fluid due to a change in the velocity gradient. Kameswaran et al. [26] investigated the hydromagnetic nanofluid flow due to a stretching or shrinking sheet with viscous dissipation and chemical reaction effects. They used the nanoparticle volume fraction model to describe the nanofluid flow problem. The radiation effect on the viscous flow of a nanofluid and heat transfer over a nonlinearly stretching sheet was studied by Hady et al. [50]. Khan et al. [51] considered the unsteady MHD free convection boundary layer flow of a viscous, incompressible nanofluid along a stretching sheet with thermal radiation and viscous dissipation effects. In most of the above studies the surface temperature is considered to be isothermal. However, there are several situations where a constant surface temperature may not be applicable. Makinde and Aziz [24] studied the boundary layer flow induced in a nanofluid due to a linearly stretching sheet.

The transport equations included the effects of Brownian motion and thermophoresis. The boundary layer flow and heat transfer of nanofluid over a vertical plate with a convective surface boundary condition was studied by Ibrahim and Shanker [52]. The investigation of boundary layer stagnation point flow of a nanofluid past a permeable flat surface with Newtonian heating was carried by Olanewaju and Makinde [53]. They used the Brownian motion and thermophoresis effects to describe the nanofluid model. There are several chemically reacting systems which involve both homogeneous and heterogeneous reactions, with examples occurring in combustion, catalysis, and biochemical systems. The interaction between the homogeneous reaction in the bulk of the fluid and heterogeneous reaction occurring on some catalytic surfaces is generally very complex, and is involved in the production and consumption of reactant species at different rates both within fluid and on the catalytic surfaces. A model for isothermal homogeneous-heterogeneous reactions in boundary layer flow of a viscous fluid past a flat plate was studied by Merkin [31]. He represented the homogeneous reaction by cubic autocatalysis and the heterogeneous reaction by a first order process and showed that the surface reaction is the dominant mechanism near the leading edge of the plate. Chaudhary and Merkin [32] investigated homogeneous-heterogeneous reactions in boundary layer flow. They obtained the numerical solution near the leading edge of a flat plate. The effects of flow near the leading edge of a flat plate. The effects of flow near the two dimensional stagnation point flow on an infinite permeable wall with a homogeneous-heterogeneous reaction were studied by Khan and Pop [35]. They solved the governing nonlinear equations using the implicit finite difference method and observed that the mass transfer parameter considerably affects the flow characteristics. Khan and Pop [36] investigated the effects of homogeneous-heterogeneous reactions on a viscoelastic fluid toward a stretching sheet. They observed that the concentration at the surface decreased with an increase in the viscoelastic parameter. Kameswaran et al. [37] investigated the homogeneous-heterogeneous reactions in a nanofluid flow due to a porous stretching sheet. They showed that the velocity profiles decrease with the fluid concentration is oppositely affected by nanoparticles volume fraction for both Cu-water and Ag-water by nanofluids. Recently, Kameswaran et al. [54] discussed the effects of homogeneous-heterogeneous reactions on stagnation point of a nanofluid over a porous stretching or shrinking sheet taking into account the effect of an externally applied magnetic field. They showed that dual solutions exists for certain suction/inject, stretching/shrinking, and magnetic parameter values. However, this study did not explain the heat transfer characteristics of the problem which is an important aspect in the flow of nanafluids. The present study aims to provides detailed discussion of the combined viscous and Joule dissipation effect on the stagnation point flow of a viscous incompressible electrically conducting nanofluid through a permeable stretching/shrinking sheet in the presence of homogeneous-heterogeneous reactions and an applied magnetic field. The nanparticle

volume fraction model is used to describe the nanofluid problem. In the present study, the density temperature relation is considered to be nonlinear which may happen due to thermal stratification and heat released by viscous dissipation and cause a nonlinear convective heat transfer. The permeable sheet is assumed to be convectively heated with a hot fluid. The governing nonlinear partial differential equations which are then solved using successive linearization method. The nanofluid problem, which is not yet considered by other researchers, finds applications in heat transfer devices where the density and temperature relations are more complex and the viscosity of the fluid has significant effect on the heat transfer rate.

3.2 Mathematical Formulation

Consider the steady two-dimensional boundary layer flow of a viscous, incompressible, and electrically conducting nanofluid in the region $y > 0$ driven by a stretching/shrinking surface at $y = 0$ with a fixed stagnation point. The fluid flow is also affected by nonlinear convection due to nonlinear temperature and density relation. Two equal but opposite force are applied along the sheet so that the wall is stretched, keeping the position of the origin unaltered. The fluid flow is permeated with a uniform transverse magnetic field B_0. It is assumed that the induced magnetic field produced by the fluid motion is negligible in comparison with the applied one. This assumption is valid for low magnetic Reynolds number fluids[11]. Also, there is no external applied electric field so that the effect of polarization of magnetic field is negligible [38]. The base fluid and the nanoparticle are in thermal equilibrium and no slip occurs between them. It is assumed that a simple homogeneous-heterogeneous reactions model exists as proposed by Chaudhary and Merkin [32] in the following form:

$$A + 2B \to 3B, \quad rate = k_c ab^2 \tag{3.1}$$

while on the catalyst surface we have the single, isothermal, first order reaction

$$A + B \to 3B, \quad rate = k_s a \tag{3.2}$$

where a and b are the concentrations of the chemical species A and B ,k_c and k_s are the rate constants. It is assumed that both the reaction processes are isothermal. Under these assumptions, the boundary layer equations describing the nanofluid flow, heat, and mass transfer can be written as

$$\frac{\partial u}{\partial x} + \frac{\partial v}{\partial y} = 0 \tag{3.3}$$

$$u\frac{\partial u}{\partial x}+v\frac{\partial v}{\partial y}=U_\infty\frac{dU_\infty}{dx}+\frac{\mu_{nf}}{\rho_{nf}}\frac{\partial^2 u}{\partial y^2}-\frac{\sigma B_0^2}{\rho_{nf}}(u-U_\infty)+g\left[\beta_{nf}(T-T_\infty)+\beta^*_{nf}(T-T_\infty)^2\right] \tag{3.4}$$

$$u\frac{\partial T}{\partial x}+v\frac{\partial T}{\partial y}=\alpha_{nf}\frac{\partial^2 T}{\partial y^2}-\frac{\sigma B_0^2}{\rho_{nf}}(u-U_\infty)^2+\frac{\mu_{nf}}{(\rho c_p)_{nf}}\left(\frac{\partial u}{\partial y}\right)^2 \tag{3.5}$$

$$u\frac{\partial a}{\partial x}+v\frac{\partial a}{\partial y}=D_A\frac{\partial^2 a}{\partial y^2}-k_c ab^2 \tag{3.6}$$

$$u\frac{\partial b}{\partial x}+v\frac{\partial b}{\partial y}=D_B\frac{\partial^2 b}{\partial y^2}+k_c ab^2 \tag{3.7}$$

where u and v are the velocity components of the nanofluid in the x- and y-directions, respectively, T is the temperature of the nanofluid, a and b are species concentration, g is the acceleration due to gravity, σ is the electrical conductivity of the nanofluid, $\mu_{nf}, \rho_{nf}, k_{nf}$ and $(c_p)_{nf}$ are, respectively, viscosity of the nanofluid, nanofluid density, nano fluid thermal conductivity, and specific heat at constant pressure. In Eq.(4), the last term accommodates the linear density temperature variation as well as the quadratic density temperature variation. In this term, β_{nf} and β^*_{nf} are the volumetric coefficients of thermal expansion of the first and second orders, respectively [47–49]. The dynamic viscosity of the nanofluid μ_{nf} was given by Brinkman [12] as

$$\mu_{nf}=\frac{\mu_f}{(1-\phi)^{2.5}} \tag{3.8}$$

where ϕ is the solid volume fraction of nanoparticles. The values of $\rho_{nf}, \beta_{nf}, (\rho c_p)_{nf}$, and α_{nf} are respectively, defined as [13]

$$\rho_{nf}=(1-\phi)\rho_f+\phi\rho_s \tag{3.9}$$

$$\beta_{nf}=\frac{\phi(\rho\beta)_s+(1-\phi)(\rho\beta)_f}{\rho_{nf}} \tag{3.10}$$

$$(\rho c_p)_{nf}=(1-\phi)(\rho c_p)_f+\phi(\rho c_p)_s \tag{3.11}$$

$$\alpha=\frac{k_{nf}}{(\rho c_p)_{nf}} \tag{3.12}$$

where k_{nf} is the thermal conductivity of the nanofluid which is given by [14, 15]

$$\frac{k_{nf}}{k_f}=\frac{k_s+2k_f-2\phi(k_f-k_s)}{k_s+2k_f+2\phi(k_f-k_s)} \tag{3.13}$$

Here, the subscripts nf, f and s refer to the thermophysical properties of the nanofluid, base fluid, and nanosolid particles, respectively. It is assumed that the surface of the sheet is stretched/shrinked with a velocity proportional to x keeping the point at the origin O as fixed. The nanofluid which is in contact with the surface of stretching/shrinking

sheet also has the same velocity because of no-slip which also causes the fluid motion near to the sheet. The free stream velocity U_∞ is assumed to be proportional to x so that there is no velocity at the point O at all. This point is known as the stagnation point of the flow. The nanofluid, which is in contact with the surface of the sheet, is convectively heated by a hot fluid which is on the other side of the sheet and whose is T_f. The temperature of the nanofluid outside the boundary layer regimes is assumed to be T_∞ Under the assumption made above the following the model for homogeneous-heterogeneous reactions proposed by Chaudary and Merkin [32], the boundary conditions for the problem are

$$u = U_x = cx, \nu = 0, -k_f \frac{\partial T}{\partial y} = h(T_f - T),$$
$$D_A \frac{\partial a}{\partial y} = k_s a, D_B \frac{\partial b}{\partial y} = -k_s a \quad \text{at} \quad y = 0, \tag{3.14}$$
$$u \to U_\infty(x) = dx, T \to T_\infty, a \to a_0, b \to 0 \quad \text{as} \quad y \to \infty \tag{3.15}$$

Introducing the following transformation:

$$\xi(x,y) = \sqrt{\nu_f U_\infty x} f(\eta), \theta = \frac{(T - T_\infty)}{T_f - T_\infty},$$
$$a = a_0 g(\eta), b = a_0 h(\eta), \eta = \sqrt{\frac{U_\infty}{\nu_f x}} y \tag{3.16}$$

where η is the dimensionless stream function and the above transformation is chosen in such a way that $u = \partial\xi/\partial y$ and $v = -\partial\xi/\partial x$. Using the above transformation, the equation of continuity (3.3) is automatically satisfied and we obtain from Eqs. (3.4)-(3.7) as

$$\frac{1}{\phi_1} f''' + f f' - f'^2 - \frac{M}{\phi_2}(f' - 1) + \frac{\lambda \phi_3}{\phi_2}\theta(1 + \alpha\theta) + 1 = 0 \tag{3.17}$$
$$\frac{\phi_4}{Pr\phi_5}\theta'' + \frac{MEc}{\phi_5}(f' - 1)^2 + \frac{Ec}{\phi_5(1-\phi)^{2.5}} f''^2 = 0 \tag{3.18}$$
$$\frac{1}{Sc} g'' + f g' - K g h^2 = 0 \tag{3.19}$$
$$\frac{\delta}{Sc} h'' + f h' + K g h^2 = 0 \tag{3.20}$$

where

$$M = \frac{\sigma B_0^2}{d\rho_f}, \lambda = \frac{g\beta_f \Delta T}{xd^2}, \alpha = \frac{\beta_{nf}^*}{\beta_{nf}}\Delta T,$$
$$Pr = \frac{\nu_f}{\alpha_f}, Ec = \frac{U_\infty^2}{\Delta T(c_p)_f}, Sc = \frac{\nu_f}{D_A}, K = \frac{k_c a_0^2}{d},$$
$$\phi_1 = (1-\phi)^{2.5}\left[(1-\phi) + \phi\left(\frac{\rho_s}{\rho_f}\right)\right]$$
$$\phi_2 = \phi_1(1-\phi)^{-2.5},$$
$$\phi_3 = \left[(1-\phi) + \phi\frac{(\rho\beta)_s}{(\rho\beta)_f}\right]$$
$$\phi_4 = \frac{k_s + 2k_f - 2\phi(k_f - k_s)}{k_s + 2k_f + 2\phi(k_f - k_s)},$$
$$\phi_5 = \left[(1-\phi) + \phi\frac{(\rho c_p)_s}{(\rho c_p)_f}\right], \qquad \delta = \frac{D_B}{D_A}$$

The nondimensional variables defined above are, the magnetic parameter M, the mixed convection parameter λ, the nonlinear density temperature (NDT) parameter α, the Prandtl number Pr, the Eckert number Ec, the Schmidt number Sc, and the homogeneous reaction rate K. The functions $\phi_1, \phi_2, \phi_3, \phi_4$,and ϕ_5 are also nondimensional and are depending upon the thermophysical properties of the nanoparticles and the base fluid. δ is the ratio of diffusion constants. The value of $\lambda > 0$ corresponds to the buoyancy assisting flow, while the value of $\lambda < 0$ corresponds to the buoyancy opposing flows and $\lambda = 0$ corresponds to the case of pure forced convection flow. The boundary conditions(3.14) and (3.15), subject to the transformation (3.16), are given by

$$f = 0, f^{'} = \varepsilon, \theta^{'} = -Bi(1-\theta), g^{'} = K_s g,$$
$$\delta h^{'} = -K_s g \quad \text{at} \quad \eta = 0 \tag{3.21}$$
$$f^{'} \to 1, \theta \to 0, g \to 1, h \to 0 \quad \text{as} \quad \eta \to \infty \tag{3.22}$$

where ε is the stretching/shrinking parameter,$Bi = (h/k_f)\sqrt{(\nu_f/d)}$ is the Biot number, and $K_s = (k_s/D_A)\sqrt{(\nu_f/d)}$ is the strength of the heterogeneous reaction. It is expected that the diffusion coefficients of chemical species A and B are of a comparable size which leads us to make a further assumption that the diffusion coefficients D_A and D_B are equal, i.e.,$\delta = 1$ [32]. This assumption leads to the following relation:

$$g(\eta) + h(\eta) = 1 \tag{3.23}$$

Equations (3.19) and (3.20) under this assumption reduce to

$$\frac{1}{Sc}g^{''} + fg^{'} - kg(1-g)^2 = 0 \tag{3.24}$$

and are subject to the boundary conditions

$$g^{'} = K_s g \quad \text{at} \quad \eta = 0, \quad \text{and} \quad g \to 1 \quad \text{as} \quad \eta \to \infty \tag{3.25}$$

The problem now reduces to the problem of solving Eqs. (3.17),(3.18), and (3.24) subject to the conditions provided in Eqs. (3.21), (3.22), and (3.25). The other physical quantities which need to be investigated are the skin friction C_f, the local Nusselt number Nu_x which may be obtained by using the following results:

$$C_f Re_x^{1/2} = \frac{1}{(1-\phi)^{2.5}} f^{''}(0) \tag{3.26}$$

$$Nu_x / Re_x^{1/2} = -\frac{k_{nf}}{k_f} \theta^{'}(0) \tag{3.27}$$

3.3 Numerical Technique

The above set of equations (3.17), (3.18) and (3.24) subject to the boundary conditions stated in (3.21), (3.22) and (3.25) were solved using Successive Linearisation Method (SLM) by Nandkeolyar et al. [55] in order to verify the robustness and applicability of Spectral Relaxation Method (SRM) we intend to apply the SRM on the problem studied by Nandkeolyar et al. [55] In view of SRM algorithm the linearised iteration scheme is given by

$$p^{''}_{r+1} + \phi_1 \left(f_{r+1} p^{'}_{r+1} - \frac{M}{\phi_2} p_{r+1} - p_r^2 \right) = 0 \tag{3.28}$$

$$\theta^{''}_{r+1} + \frac{Prk_f}{k_{nf}} \left(f_{r+1} \theta^{'}_{r+} - 2 f^{'}_{r+1} \theta_{r+1} + \frac{\beta}{\phi_3} \theta_{r+1} \right) = 0 \tag{3.29}$$

$$\frac{1}{Sc} g^{''}_{r+1} + f_{r+1} g^{'}_{r+1} - K g_{r+1} = K(g_r^3 - 2g_r^2) \tag{3.30}$$

The boundary conditions for the above iteration scheme are

$$f_{r+1} = 0, f^{'}_{r+1} = \epsilon, \theta^{'}_{r+1} = -Bi(1 - \theta_{r+1}), g^{'}_{r+1} = K_s g_{r+1},$$
$$\delta h^{'}_{r+1} = -K_s g_{r+1} \quad \text{at} \quad \eta = 0$$
$$f^{'}_{r+1} \to 1, \theta_{r+1} \to 0, g_{r+1} \to 1, h_{r+1} \to 0 \quad \text{as} \quad \eta \to \infty$$
$$g^{'}_{r+1} = K_s g_{r+1} \quad \text{at} \quad \eta = 0, \quad \text{and} \quad g_{r+1} \to 1 \quad \text{as} \quad \eta \to \infty$$

In order to solve the decoupled equations (3.28)-(3.30), we use the Chebyshev spectral collocation method. The computational domain $[0, L]$ is transformed to the interval $[-1, 1]$ using $\eta = L(\xi + 1)/2$ on which the spectral method is implemented. Here L

is used to invoke the boundary condition at ∞. The basic idea behind the spectral collocation method is the introduction of a differentiation matrix $\mathcal{D}$ which is used to approximate the derivatives of the unknown variable at the collocation points as the matrix vector product of the form

$$\frac{df_{r+1}}{d\xi} = \Sigma_{k=0}^{N} \mathbf{D}_{lk} f_r(\eta_k) = \mathbf{D}\mathbf{f}_r, l = 0, 1, 2, ..., N \tag{3.31}$$

where $N+1$ is the number of collocation points (grid points), $\mathbf{D} = 2\mathcal{D}/L$, and $f = [f(\eta_0), f(\eta_1, ..., f(\eta_N)]^T$ is the vector function at the collocation points. Higher-order derivatives obtained as poers of D, that is,

$$f_r^{(p)} = \mathbf{D}^p \mathbf{f}_r, \tag{3.32}$$

where p is the order of the derivative. Applying the spectral method to equations (3.28)-(3.30) we obtain

$$A_1 f_{r+1} = B_1 \tag{3.33}$$

$$A_2 p_{r+1} = B_2 \tag{3.34}$$

$$A_3 \theta_{r+1} = B_3 \tag{3.35}$$

$$A_4 g_{r+1} = B_4 \tag{3.36}$$

where

$$\begin{aligned} A_1 &= \mathbf{D} \\ B_1 &= p_r \end{aligned} \tag{3.37}$$

$$\begin{aligned} A_2 &= diag\left(\frac{1}{\phi_1}\right)\mathbf{D}^2 + diag(f_{r+1})\mathbf{D} + diag\left(\frac{M}{\phi_2}\right) I \\ B_2 &= p_r^2 - \frac{M}{\phi_2} - \frac{\lambda\phi_3\theta_r}{\phi_2} - 1 \end{aligned} \tag{3.38}$$

$$\begin{aligned} A_3 &= diag\left(\frac{\phi_4}{Pr\phi_5}\right)\mathbf{D}^2 + diag(f_{r+1})\mathbf{D} \\ B_3 &= -\frac{MEc}{\phi_5}(p_r - 1)^2 - \frac{Ecp_r'^2}{\phi_5(1-\phi)^{2.5}} \end{aligned} \tag{3.39}$$

$$\begin{aligned} A_4 &= diag\left(\frac{1}{Sc}\right)\mathbf{D}^2 + diag(f_{r+1})\mathbf{D} - diag(k)I \\ B_4 &= K(g_r^3 - 2g_r^2) \end{aligned} \tag{3.40}$$

In equations(3.37)-(3.40) , I is an identity matrix and diag[ ] is a diagonal matrix, all of size $(N+1)\times(N+1)$ where N is the number of grid points,$\mathbf{f}, \mathbf{p}, \theta$ and $\mathbf{g}$ are the values of the functions f, p, θ and g respectively, when evaluated at the grid points and the subscript r denotes the iteration number. The initial guesses to start the SRM scheme

for equation (3.28)-(3.30) are chosen as

$$f(\eta) = \eta + e^{-\eta} - e^{-\epsilon\eta}, \theta(\eta) = \frac{1}{2}e^{-Bi\eta}, g(\eta) = 1 - 0.5e^{-K_s\eta} \tag{3.41}$$

3.4 Numerical Results

In order to study the efficiency of the spectral relaxation method on the present problem, the values of skin friction coefficient $-f''(0)$, heat transfer coefficient $-\theta'(0)$, and $g'(0)$ were calculated and compared with the old values reported by Nandkeolyar et al. [55]. These values are reported in Tables 3.1 and 3.2 and exhibit very good agreement with the results of Nandkeolyar et al. [55]. The effect of increase in the values or M, ϕ, and α, on the skin friction, which is proportional to $f^{''}(0)$, and the Nusselt number which measures the rate of heat transfer at the plate and can be measured as a variation in $\theta^{'}(0)$, are presented Table 3.2. It is observed that an increase in the magnetic field causes an increase in the skin friction, whereas an opposite effect on the skin friction is encountered with an increase in nonlinear density-temperature relation and viscous dissipation. An increase in the nanoparticle volume fraction tends to increase the skin friction first and then it tends to decrease it. Thus by increasing the nanoparticle volume fraction, one can obtain a higher heat transfer with lesser skin friction. The rate of heat transfer at the surface decrease with an increase in the Joule dissipation, nanoparticle volume fraction, viscous dissipation, and stretching rate, whereas it is oppositely affected by nonlinear density-temperature relation and convective heat transfer.

3.5 Conclusions

However there are several numerical techniques such as Shooting technique, finite difference methods, Keller-box method, and some other softwares to attack the problems arising in fluid dynamics, the use of spectral relaxation methods is much desired due to the robustness and fast convergence of these methods. Shooting techniques has a serious disadvantage that the numerical computation is based on the initial guesses to satisfy certain boundary conditions which sometime becomes impossible. The technique has to be coupled with some initial values problem solver technique to be applied on certain boundary value problems. Keller-box method, on the other hand, is more or less a finite difference scheme and the application of the on even a simple fluid dynamic problem becomes very tedious. Moreover, the error minimization in this method becomes very difficult and requires a careful discretization which turn requires more effort and CPU time. The overall advantage of spectral methods is that these are easy to implement,

requires less number of iterations, and further these are not that much sensitive to the discretization process. The spectral methods start with initial guesses for the unknown variables which are simply convenient functions satisfying the boundary conditions.

TABLE 3.1: Comparision of SLM results and present results for various values of magnetic parameter M when $\phi = 0.2, \lambda = 1, \alpha = 0.2, Bi = 5, \varepsilon = 2, Sc = 1, K_s = 0.5$ and $Ec = 0.1$

	SLM results			SRM results		
M	$-f''(0)$	$-\theta'(0)$	$g'(0)$	$-f''(0)$	$-\theta'(0)$	$g'(0)$
0	2.19048061	0.99333458	0.3243352	2.19048061	0.99333458	0.3243352
0.5	2.25028011	0.9570171	0.3295434	2.25028011	0.9570171	0.3295434
1	2.30871894	0.92166934	0.3268613	2.30871894	0.92166934	0.3268613
1.5	2.36588096	0.88722548	0.32342816	2.36588096	0.88722548	0.32342816
2	2.42184215	0.85362629	0.32317974	2.42184215	0.85362629	0.32317974
2.5	2.47667158	0.82081836	0.32294027	2.47667158	0.82081836	0.32294027

TABLE 3.2: Effects of various parameters on coefficient of skin friction and Nusselt number when $\lambda = 1, K = 0.5, K_s = 0.5,$ and $Sc = 1$

				SLM results		SRM results	
M	ϕ	A	Ec	$-f''(0)$	$-\theta'(0)$	$-f''(0)$	$-\theta'(0)$
2	0.2	0.2	0.1	2.42184215	0.85362629	2.421842	0.853626
6	-	-	-	2.83346802	0.60975651	2.833468	0.609756
10	-	-	-	3.1962013	0.39883347	3.19620	0.398833
-	0.1	-	-	2.40489475	1.05127874	2.404895	1.051278
-	0.2	-	-	2.42184215	0.85362629	2.421842	0.853626
-	0.3	-	-	2.3084809	0.67790312	2.30848	0.677903
-	-	0	-	2.43376169	0.85161072	2.433762	0.851610
-	-	1	-	2.37444335	0.86154383	2.374443	0.861543
-	-	2	-	2.31579755	0.87112526	2.315798	0.871125
-	-	-	0	2.44927467	1.41282824	2.449275	1.412828
-	-	-	1	2.14974639	-3.61464877	2.149746	-3.614648
-	-	-	2	1.81679305	-7.44221797	1.816793	-7.442217

Bibliography

[1] R. Nandkeolyar, P. Kameswaran, S. Shaw, and P. Sibanda. Heat transfer on nanofluid flow with homogeneous-heterogeneous reactions and internal heat generation. *Heat Transfer*, 2014.

[2] S. U. S. Choi. Enhancing thermal conductivity of fluids with nanoparticles. *Proceedings of the 1995 ASME Int. Mech. Eng. Cong. and Exposition, San Francisco, USA*, ASME FED 231/MD 66:99–105, 1995.

[3] S. U. S. Choi, Z. G. Zhang, W. Yu, F. E. Lockwood, and E. A. Grulke. Anomalously thermal conductivity enhancement in nanotube suspensions. *Appl. Phys. Lett.*, 79: 2252–2254, 2001.

[4] S. U. S. Choi. Nanofluids: from vision to reality through research. *J. Heat Transf.*, 131(3):1–9, 2009.

[5] W. Yu, D. M. France, J. L. Routbort, and S. U. S. Choi. Review and comparison of nanofluid thermal conductivity and heat transfer enhancements. *Heat Transf. Eng.*, 29(5):432–460, 2008.

[6] T. Tyler, O. Shenderova, G. Cunningham, G. Walsh, J. Drobnik, and G. McGuire. Thermal transport properties of diamond-based nanofluids and nanocomposites. *Diamond and Related Materials*, 15(11-12):2078–2081, 2006.

[7] S. R. Das, S. U. S. Choi, and H. E. Patel. Heat transfer in nanofluidsa review. *Heat transf. eng.*, 27(10):3–19, 2006.

[8] M. S. Liu, M. C. C. Lin, I. T. Huang, and C. C. Wang. Enhancement of thermal conductivity with carbon nanotube for nanofluids. *Int. Comm. Heat Mass Transf.*, 32(9):1202–1210, 2005.

[9] S. U. S. Choi, Z. G. Zhang, and P. Keblinski. Nanofluids, in encyclopedia of nanoscience and nanotechnology. *American Scientific*, 6:757–737, 2004.

[10] C. G. Granqvist and R. A. Buhrman. Ultrafine metal particles. *Journal of Applied Physics*, 47(5):2200–2219, 1976.

[11] K. R. Cramer and S. I. Pai. *Magnetofluiddynamics for Engineers and Applied physicists*. McGraw Hill Book Company, New York, 1973.

[12] H. C. Brinkman. The viscosity of concentrated suspensions and solution. *J. Chem. Phys.*, 20:571–581, 1952.

[13] S. M. Aminossadati and B. Ghasemi. Natural convection cooling of a localized heat source at the bottom of a nanofluid-filled enclosure. *European J. Mech. B/Fluids*, 28(2):630–640, 2009.

[14] J. C. M. Garnett. Colours in metal glasses and in mettaillic fielms. *Philos. Trans. R. Soc. Lond. A*, 203:385–420, 1904.

[15] C. A. Guérin, P. Mallet, and A. Sentenac. Effeffect-medium theory for finite-size aggregates. *J. Opt. Soc. Am. A*, 23(2):349–358, 2006.

[16] H. Masuda, A. Ebata, K. Teramae, and N. Hishinuma. Alteration of thermal conductivity and viscosity of ofliquids by dispersing ultra-fine particles. *Netsu Busse.*, 7:227–233, 1993.

[17] Y. Xuan, Li, and Q. Heat transfer enhancement of nanofluids. *Heat Fluid Flow,21(1),pp.58-64*, 2000.

[18] Yoo, D H, Hong, K.S, Yang, and H.S. Study of thermal conductivity of nanofluids for the application of heat transfer fluids. *Thermochim.Acta,455(1-2),pp 66-69*, 2007.

[19] Hu, P, Shan, W.L, Yu, F, Chen, and Z.S. Thermal conductivity of ain- ethanol nanofluid. *Int Thermphys,29(6) ,pp 1968-1973*, 2008.

[20] W. J. Minkowycz, E. M. Sparrow, and J. P. Abraham. *Nanoparticle Heat Transfer and Fluid Flow*. CRC Press, 2012.

[21] H. U. Kang, S. H. Kim, and J. M. Oh. Estimation of thermal conductivity of nanofluid using experimental effective particle volume. *Exp. Heat Transf.*, 19(3): 181–191, 2006.

[22] V. Velagapudi, R. K. Konijeti, and C. S. K. Aduru. Empirical correlation to predict thermothermop and heat transfer characteristics of nnanofluid. *Therm. Sci.*, 12(2): 27–37, 2008.

[23] V. Y. Rudyak, A. A. Belkin, and E. A. Tomilina. On the thermal conductivity of nnanofluids. *Tech. Phys. Lett.*, 36(7):660–662, 2010.

[24] O. D. Makinde and A. Aziz. Boundary layer flow of a nanofluid past a stretching sheet with a convective boundary condition. *Int. J. Thermal Sci.*, 50:1326–1332, 2011.

[25] M. Narayana and P. Sibanda. Laminar flow of a nanoliquid film over an unsteady stretching sheet. *Int. J. Heat Mass Transf.*, 55:7552–7560, 2012.

[26] P. K. Kameswaran, M. Narayana, P. Sibanda, and P. V. S. N. Murthy. Hydromagnetic nanofluid flow due to a stretching or shrinking sheet with viscous dissipation and chemical reaction effect. *Int. J. Heat Mass Transf.*, 55:7587–7595, 2012.

[27] M. A. A. Hamad and I. Pop. Unsteady MHD free convection flow past a vertical permeable flat plate in a rotating frame of reference with constant heat source in a nanofluid. *Heat Mass Transfer.*, 47:1517–1524, 2011.

[28] M. A. A. Hamad and I. Pop. Scaling transformations for boundary layer flow near the stagnation-point on a heated permeable stretching surface in a porous medium saturated with a nanofluid and heat generation/absorption effects. *Transp Porous Med*, 87:25–39, 2011.

[29] A. J. Chamkha and A. M. Aly. MHD free convection flow of a nanofluid past a vertical plate in the presence of heat generation or absorption effects. *Chem. Eng. Comm.*, 198:425–441, 2011.

[30] A. Alsaedi, M. Awais, and T. Hayat. Effects ofheat generation/absorption on stagnation point flow of nanofluid over a surface with convective boundary conditions. *Comm. Nonliear. Sci. Numer. Simulat.*, 17:4210–4223, 2012.

[31] J. H. Merkin. A model for isothermal homogeneous-heterogeneous reactions in boundary layer flow. *Math. Comput. Model.*, 24(8):125–136, 1996.

[32] M. A. Chaudhary and J. H. Merkin. A simple isothermal model for homogeneous-heterogeneous reactions in boundary layer flow: II. different diffusivities for reactant and autocatalyst. *Fluid Dynam. Res.*, 16:335–359, 1995.

[33] Z. Ziabakhsh, G. Domairry, H. Bararnia, and H. Babazadeh. Analytical solution of flow and diffusion of chchemical reactive species over a nononlinear stretching sheet immersed in a porous medium. *J. Taiwan Inst. Chem. Eng.*, 41:22–28, 2010.

[34] P. L. Chambre and A. Acrivos. On chemical surfaces reactions in laminar boundary layer flows. *J. Appl. Phys.*, 27:1322–1328, 1956.

[35] W. A. Khan and I. Pop. Flow near the two-dimensional stagnation point on a infinite permeable wall with a homogeneous-heterogeneous reaction. *Comm. Nonliear. Sci. Numer. Simulat.*, 15:3435–3443, 2010.

[36] W. A. Khan and I. Pop. Effect of homogeneous-heterogeneous reactions on the visco-elastic fluid towards a stretching sheet. *ASME J. Heat Transf.*, 134:064506 1–5, 2012.

[37] P. K. Kameswaran, S. Shaw, P. Sibanda, and P. V. S. N. Murthy. Homogeneous-heterogeneous reactions in a nanofluid flow due to a porous stretching sheet. *Int. J. Heat Mass Transf.*, 57:465–472, 2013.

[38] R. C. Meyer. On reducing aerodynamic heat-transfer rates by magnetohydrodynamic techniques. *J. Aero. Sci.*, 25:561–572, 1958.

[39] W. Ibrahim, B. Shankar, and M. M. Nandeppanavar. MHD stagnation poiont flow and heat transfer due to nanofluid towards a stretching sheet. *Int. J. Heat Mass Transf.*, 56:1–9, 2013.

[40] A. J. Chamkha, A. M. Rashad, and E. Al-Meshaiei. Melting effect on unsteady hydromagnetic flow of a nanofluid past a stretching sheet. *Int. J. Chem. Reactor Eng.*, 9:A113, 2011.

[41] O. Anwar Bég, M. S. Khan, Ifsana Karim, Md. M. Alam, and M. Ferdows. Explicit numeruical study of unsteady hydromagnetic mixed convective nanofluid flow from an exponentially stretching sheet in porous media. *Appl. Nanosci.*, 2013. doi: 10.1007/s13204-013-0275-0.

[42] A. V. Kuznetsov and D. A. Nield. Natural convective boundar-layer flow of a nanofluid past a vertical plate. *Int. J. Thermal Sci.*, 49:243–247, 2010.

[43] K. Das. Mixed convection stagnation point flow and heat transfer of cu-water nanofluids towards a shrinking sheet. *Heat Trans. Asian Res.*, 42(3):230–242, 2013.

[44] Hossein Ali Pakravan and Mahmood Yaghoub. Combined thermophoresis, brownian motion and dufour effects on natural convection of nanofluids. *Int. J.of Thermal Sci.*, 50(3):394–402, 2011.

[45] A. V. Kuznetsov and D. A. Nield. Double-diffusive natural convective boundar-layer flow of a nanofluid past a vertical plate. *Int. J. Thermal Sci.*, 50:712–717, 2011.

[46] M. K. Partha. Nonlinear convection in a non-darcy porous medium. *Appl. Math. Mech.*, 31(5):565574, 2010. doi: 10.1007/s10483-010-0504-6.

[47] H. Barrow and T. L. S. Rao. The effect of variable beta on free convection. *Br. Chem. Eng.*, 16:704–709, 1971.

[48] A. Brown. The effect of laminar free convection heat transfer of the temperature dependence of the coefficient of volumetric expansion. *J. Heat Transf.*, 97:133–135, 1975.

[49] K. V. Prasad, K. Vajravelu, and Rober A. van Gorder. Non-darcian flow and heat transfer along a permeable vertical surface with nonlinear density temperature variation. *Acta Mech.*, 220:139–154, 2011.

[50] F. M. Hady, F. S. Ibrahim, S. M. Abdel-Gaied, and Mohamed R. Eid. Radiation effect on viscous flow of a nanofluid and heat transfer over a nonlinearly stretching sheet. *Nanoscale Research Letters*, 7:229, 2012.

[51] Md. S. Khan, I. Karim, L. E. Ali, and A. Islam. Unsteady MHD free convection boundary-layer flow of a nanofluid along a stretching sheet with thermal radiation and viscous dissipation effects. *Int. Nano Letters*, 2(24):1–9, 2012. doi: 10.1186/2228-5326-2-24.

[52] W. Ibrahim and B. Shanker. Boundary-layer flow and heat transfer of nanofluid over a vertical plate with convective surface boundary condition. *J. Fluids Eng.*, 134(8):0812031–8, 2012. doi: 10.1115/1.4007075.

[53] A. M. Olanrewaju and O. D. Makinde. On boundary layer stagnation point flow of a nanofluid over a permeable flat surface with newtonian heating. *Chem. Eng. Comm.*, 200:836–852, 2013.

[54] P. K. Kameswaran, P. Sibanda, C. RamReddy, and P. V. S. NMurthy. Dual solutions of stagnation-point flow of a nanofluid over a stretching surface. *Boundary Value Problems*, 2013:1–12, 2013.

[55] R. Nandkeolyar, S. S. Motsa, and P. Sibanda. Viscous and joule heating in the stagnation point nanofluid flow through a stretching sheet with homogenousheterogeneous reactions and nonlinear convection. *J. Nanotech. Eng. Med.*, 4:04100 1–9, 2013.